

Deformation Kinetics of Polypropylene Hollow Fibers in a Continuous Drawing Process

MOO SEOK LEE,¹ TAE HWAN OH,¹ SANG YONG KIM,¹ HYUN JOO SHIM²

¹ Department of Fiber & Polymer Science, College of Engineering, Seoul National University, San 56-1, Shinlim-Dong, Kwanak-Ku, Seoul 151-742, South Korea

² Department of Textile Engineering, Soongsil University, Seoul, South Korea

Received 19 February 1999; accepted 14 March 1999

ABSTRACT: Effects of isothermal drawing conditions on the deformation kinetics and dimensional change of polypropylene (PP) hollow fibers in a continuous drawing process were investigated. The deformation behavior of solid PP polymers during stretching between two rolls in the isothermal bath was analyzed by a simple model describing the continuous drawing process with a constitutive relation that can express a true (stress–strain–strain rate) surface of solid semicrystalline polymers. Necking profiles during drawing can be calculated from this model without any special assumption for neck criterion, and the calculated results predict that the localization of deformation is promoted with the increase of applied draw ratios. It is also found that at 20°C, the neck is observed apparently both from the calculated and experimental results, and the strain-rate sensitivity parameter is considered to be a critical factor that determines the intensity of the neck geometry. The calculated drawing forces are shown to increase with increasing the applied draw ratio and decreasing the drawing temperature, and these trends were verified by experimental results. The hollowness, defined as the ratio of inner to total cross-sectional area, increases as it is drawn at 30°C, but decreases as drawn above this temperature compared with that of the undrawn fiber. © 1999 John Wiley & Sons, Inc. *J Appl Polym Sci* 74: 1836–1845, 1999

Key words: hollow fiber; continuous drawing; strain-rate sensitivity; polypropylene; necking

INTRODUCTION

In the manufacture of some polymeric products, the polymers in the solid or molten state are sometimes subjected to a large stretch. For example, in the melt-spinning and drawing process, polymers are deformed by the difference between feeding and take-up velocities. Although both of them are the same continuous operation, there are some differences in the deformation kinetics

of these two processes because of their rheological properties.

Melt spinning is a kind of technique to manufacture hollow fibers,¹ and it is usually followed by a drawing process in a consecutive or separate operation. In the drawing of hollow fibers, not only are the drawing force and stress distributed along the drawing path, which affect the microstructure of fibers of particular interest, but also the profile development and hollowness of the final drawn fiber are of significant value. The cold stretching of melt-spun polypropylene hollow fiber is particularly important for its special end uses such as membranes.² In our previous study,³ the melt-spinning process for hollow fibers was numerically simulated, and the dynamics of melt

Correspondence to: M. S. Lee.

Contract grant sponsor: Research Fund for Advanced Materials (Ministry of Education, The Republic of Korea).

Journal of Applied Polymer Science, Vol. 74, 1836–1845 (1999)

© 1999 John Wiley & Sons, Inc.

CCC 0021-8995/99/071836-10

spinning and profile development of hollow fibers were reported. These results can give a more detailed understanding of the difference between the deformation mechanisms of the melt-spinning and drawing processes.

The analysis of deformation behavior is essential to understand the correlation between process conditions and final properties. Thus, a number of researchers have attempted to elucidate the deformation mechanism of polymers during stretching processes. Particularly, in some articles,⁴⁻⁷ the mathematical models describing the melt-spinning process have been solved with the aid of a numerical techniques. On the other hand, there have been relatively few studies aimed at the modeling of large plastic deformation in a continuous drawing process, despite its industrial significance. The main factor that makes such an analysis more difficult than in the case of melt spinning is that there has been no satisfactory constitutive relation that describes the rheological behavior of the solid polymers.

Roll drawing or continuous drawing is often termed "constant-force drawing," because the drawing force along the drawing line is constant if drag and inertia forces are neglected.⁸⁻¹⁰ From this viewpoint, a creep test can simulate the continuous stretching between rolls. Le Bourvellec et al.^{9,11} have explained the deformation kinetics of continuous drawing from creep tests, and analyzed structural development under a constant load. Salem found that the microstructure development during the constant-force roll drawing showed some differences from that of a constant rate of the extension test due to its characteristic deformation behavior.¹⁰ In the present work, to find out optimum process conditions for the manufacture of polypropylene hollow fibers, a simple model describing a continuous drawing process is presented. A constitutive relation for solid semi-crystalline polymers was used in this model, for which parameters can be determined by tensile tests.¹²⁻¹⁴ Calculations were carried out to predict the trends of strain localization as a function of the drawing conditions under an isothermal condition. The effects of drawing conditions on hollowness and drawing force are also discussed from these results.

EXPERIMENTAL

Preparation of Hollow Fibers

The polymeric material used in this study was textile-grade isotactic polypropylene (PP), with a

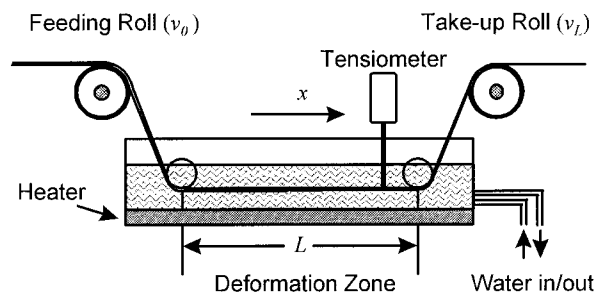


Figure 1 Schematic description of drawing system with isothermal bath.

molecular weight (M_n) of 36,900. For the preparation of the undrawn hollow fiber, PP was melt spun through a spinneret that consisted of four segmented arcs. A melt-spinning system manufactured by Uenoyama Kiko Co. was used for the laboratory-scale experiment, and a water quenching box was used for quenching conditions.

Drawing

The drawing apparatus consists of a feed roll, water bath, take-up roll, and tensiometer, as illustrated in Figure 1. Tension of the running filament was measured at a fixed position with a pin-type tensiometer that has a reading display with the capability of averaging the consecutive data. Measurement was taken by ensuring that the head of the tensiometer made direct contact with the filament in the water bath, which was controlled to maintain constant temperature. To investigate neck profiles, the part of the filament that shows the most remarkable reduction in diameter was cut from the filament in the drawing line, and its outer diameter profile was obtained by image analysis. Drawing experiments were carried out in this work under various conditions, as listed in Table I.

Hollowness Measurement

To estimate the relative quantity of the hollow portion of the fiber, hollowness, defined as the ratio of area of the hollow portion to the total cross-sectional area, was measured. Hollow fibers were cut with a microtome to prepare cross-sections, and hollowness was determined using an image analysis system with a built-in microscope.

FORMULATION AND CALCULATION

To develop a mathematical model for the deformation in the continuous drawing system shown

Table I Drawing Conditions of PP Hollow Fibers

Draw Ratio Effect (20 and 80°C)			Drawing Velocity Effect (80°C)			Drawing Temperature Effect (°C)	
v_0 (m/min)	v_L (m/min)	DR	v_0 (m/min)	v_L (m/min)	DR	$v_0 = 5$ m/min, $v_L = 25$ m/min)	
5	20	4	3	15	5	20	60
5	25	5	6	30	5	30	70
5	30	6	9	45	5	40	80
			12	60	5	50	90

in Figure 1, the following assumptions were made: plug flow was assumed as employed in some studies,^{15,16} so that deformation is considered to be perfectly extensional, and this makes it possible to develop one-dimensional formulations. As stated in our previous article,³ hollow fibers inherently need two-dimensional analysis to predict inner- and outer-diameter profiles. However, area change and other variables along the drawing path such as strain, strain rate, and stress can be calculated by one-dimensional formulation. For isothermal conditions, a water bath with a temperature-control unit was used in this drawing system, and because water is highly efficient in transferring the heat, it can be assumed that the filament holds an ambient water temperature in the water bath. Deformation of filaments was assumed to occur only in the heating zone, and this was confirmed by observing no detectable reduction in the diameter outside the heating zone. Fiber failure at higher levels of the drawing stresses was not considered in this calculation. As well as constant force along drawing path, incompressibility of the fiber and steady-state drawing were assumed.

Applying the conservation of mass and momentum with application of rheological properties of solid polymers, we obtain the following expressions:

$$\rho Av = W = \text{const.} \quad (1)$$

$$F = \sigma A = \text{const.} \quad (2)$$

$$\sigma = k[1 - \exp(-\omega\varepsilon)]\exp(h\varepsilon^2)(\dot{\varepsilon}/\dot{\varepsilon}_0)^m \quad (3)$$

where A , v , and F denote the area, axial velocity, and tensile force, respectively; σ is the true stress, ε the true strain, and $\dot{\varepsilon}$ the true strain rate of filament at a distance, x from the feed roll; $\dot{\varepsilon}_0$, ρ ,

and W are the reference strain rate (conventionally equal to 1 s^{-1}), density, and mass flow rate, respectively; k , h , ω , and m are the rheological parameters at a given temperature, each denoting the scaling factor, strain-hardening factor, viscoelastic coefficient, and strain-rate sensitivity coefficient respectively. In eq. (3), $[1 - \exp(-\omega\varepsilon)]$ represents the viscoelastic term, $\exp(h\varepsilon^2)$ expresses the strain-hardening effect at the large stretch, and the term $(\dot{\varepsilon}/\dot{\varepsilon}_0)$ describes the strain-rate sensitivity. More details on the constitutive relations are given elsewhere.¹²⁻¹⁴

The boundary conditions for velocity on both ends of the drawing line are:

$$v(0) = v_0$$

$$v(L) = v_L \quad (4)$$

where v_0 and v_L are the feed roll and take-up roll velocity, respectively.

For the development of equations in terms of local variables of the continuous drawing process, the local true strain and strain rate at a position x can be expressed as follows:

$$\varepsilon = \ln\left(\frac{l}{l_0}\right) = \ln\left(\frac{v}{v_0}\right) \quad (5)$$

$$\dot{\varepsilon} = v \frac{d\varepsilon}{dx} \quad (6)$$

where l is the current length of the filament element and l_0 its initial value.

Combining the above equations gives displacement x from the feed roll as a function of the local true strain:

Table II Rheological Parameters of PP Used in This Calculation

Temperature (°C)	k (MPa)	h	m	ω
20	63	0.56	0.03	35
80	17	0.55	0.06	32

$$x = \frac{v_0}{\dot{\varepsilon}_0} \left(\frac{k}{\sigma_0} \right)^{1/m} \int_0^\varepsilon R(\varepsilon) d\varepsilon \quad (7)$$

where

$$R(\varepsilon) = \exp(\varepsilon) [\exp(h\varepsilon^2 - \varepsilon) - \exp(h\varepsilon^2 - (\omega + 1)\varepsilon)]^{1/m} \quad (8)$$

From eq. (7) with boundary conditions, a plot of ε against x can be obtained by numerical integration. The range of the strain from zero to maximum value, ε_L , which corresponds to the applied draw ratio, must be sectioned into fine elements for numerical integration of eq. (7). Using some of the relations presented above, other variables along the axial distance can also be computed.

In the present calculation, the rheological parameters for polypropylene were assigned with regard to two drawing temperatures, as listed in Table II. Some parameters were so sensitive that they were carefully selected for successful simulation of the continuous drawing system. The parameters with respect to temperature were chosen for their temperature dependence to follow the trends of G'Sell's work.¹²

RESULTS AND DISCUSSION

Deformation kinetics was calculated under conditions shown in Table I that were used in actual experiments to simulate an isothermal continuous drawing system. To understand the deformation history of filaments during their transfer from the feed roll to the take-up roll in continuous drawing, we can consider the filament elements along the axial distance, which are under a different deformation state. Because each element is considered to follow the governing equations and constitutive relation, we can obtain the local variables at each position along the drawing line by solving the equations. The results are shown in

Figure 2, and from these, the characteristics of continuous drawing can be found. Overall features of profiles are similar to those in melt spinning, because both the spinning and drawing processes are the same continuous operation between two rolls. The fiber elements in both processes are accelerated from their initial to fi-

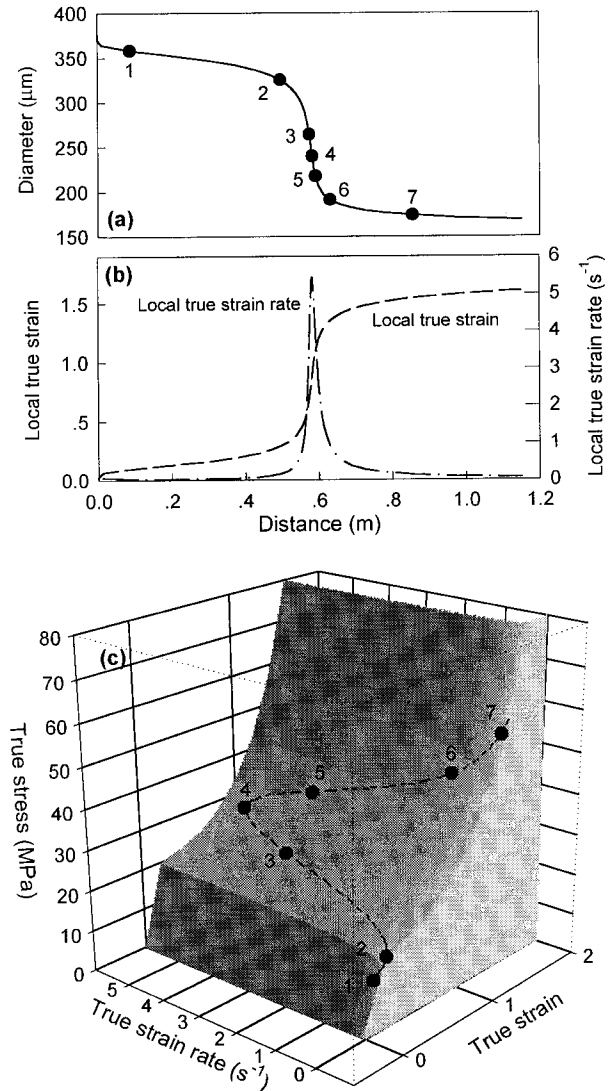


Figure 2 Calculated deformation history described in terms of local variables along drawing line for the continuous drawing (drawing temperature: 80°C; applied draw ratio: 5): (a) diameter profile; (b) local true strain and strain rate profile; (c) true (stress–strain–strain rate) surface at the temperature 80°C and the deformation path of the fiber elements on the drawing line. Several points are numbered for describing that the fiber element at some position of the drawing line can be mapped onto corresponding points of the true (stress–strain–strain rate) surface.

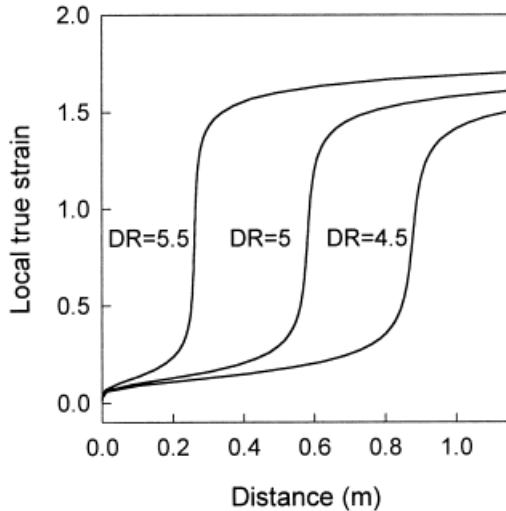


Figure 3 The calculated local true strain profile along the drawing line for a continuous drawing of PP hollow fibers at various applied draw ratios ($T = 80^{\circ}\text{C}$).

nal take-up velocity, and velocity or strain profile has a sigmoidal shape with an inflexion point and a horizontal asymptote at the end of the deformation zone. The strain rate, thus, has a maximum in both cases. However, the strain in the drawing process is localized more intensively, and a neck appears by drastic reduction of the diameter that cannot, in general, be found in melt spinning.

Figure 2(a) exhibits a neck profile that is predicted by solving the equations presented above without any special assumption for neck criterion. Running fiber elements during drawing deform continuously under different states of true stress, strain, and strain rate at each position x . The fiber element under consideration can be represented by a single point on the true (stress-strain-strain rate) surface at a given temperature. It is shown that the points in Figure 2(a) can be mapped onto corresponding points in the true σ - ϵ - $\dot{\epsilon}$ surface in Figure 2(c), and this makes it possible to understand that the fiber elements go through the deformation from the linear elastic to the strain-hardening region under this drawing condition. The interaction of these various stress states results in strain localization or necking. For example, the fiber elements near the points numbered 1 and 7 in Figure 2(a) are mapped to the initial elastic region and the strain-hardening region in Figure 2(c). In these regions, a large increase of stress is required for a small change in the strain, so that the deformation in the initial and final regions of continuous drawing is not

activated. On the other hand, near the points numbered 3, 4, and 5, a small increase of stress causes a large strain, as shown in the true σ - ϵ - $\dot{\epsilon}$ surface, and this leads to strain localization.

The applied draw ratio is determined by the ratio of initial to final velocity of the filament. It is illustrated in Figures 3 through 6 that the applied draw ratio affects the local history of deformation, which results in a change in deformation kinetics. The position of strain localization (i.e., position of a steep increase of the local true strain in Fig. 3) shifts towards the lower strain region with increasing the draw ratio. It may also be understood from Figures 4 and 5 that the intensity of the strain localization increases with the draw ratio by noticing the rise of the maximum strain rate and slope of the area reduction. The change in the local true strain rate with respect to the applied draw ratio is illustrated in Figure 4. We often estimate the effects of the strain rate in the drawing by the average or initial strain rate.^{10,17} However, in a continuous drawing, it is necessary to consider a local change of strain rate because of its large local variation, especially for a high applied draw ratio.

As is well known, an increase of the draw ratio promotes the development of the structure of the drawn fibers. This fact can be explained by results whereby the filaments are stretched under a larger stress due to a strain-hardening effect at a higher applied draw ratio, as shown in Figure 6.

To investigate the effects of drawing temperature, calculations were performed for two drawing

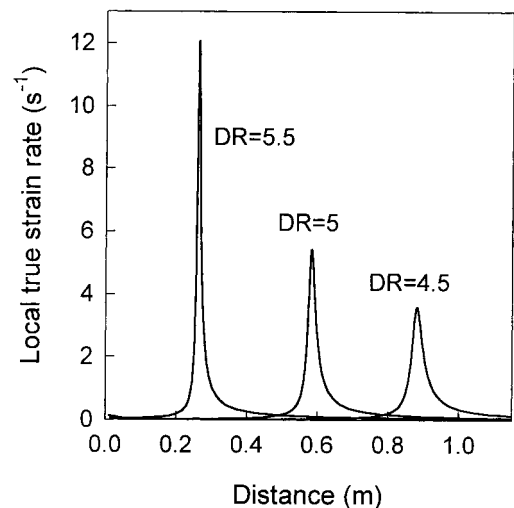


Figure 4 The calculated local true strain rate profile along the drawing line for a continuous drawing of PP hollow fibers at various applied draw ratios ($T = 80^{\circ}\text{C}$).

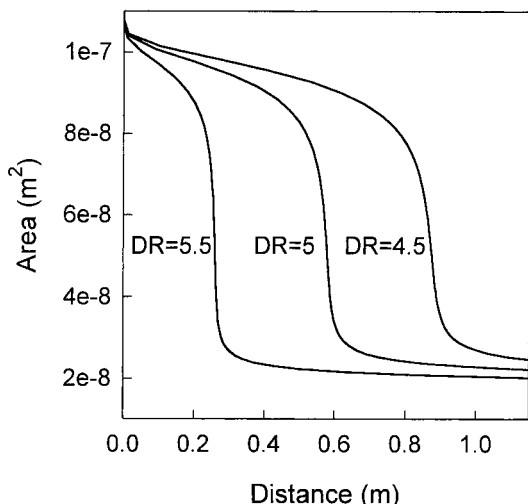


Figure 5 The calculated area profile along the drawing line for a continuous drawing of PP hollow fibers at various applied draw ratios ($T = 80^{\circ}\text{C}$).

temperatures, in which noticeable differences in deformation behavior could be observed. Such differences with respect to drawing temperatures result from the dependence of rheological parameters on temperature, and they determine the true σ - ε - $\dot{\varepsilon}$ surface that affects the drawing behaviors. From Figures 7 and 8, it can be seen that the deformation localization at a lower drawing temperature is more remarkable than at a higher temperature. It should be noted that no drastic change of strain is exhibited at 80°C in a practical

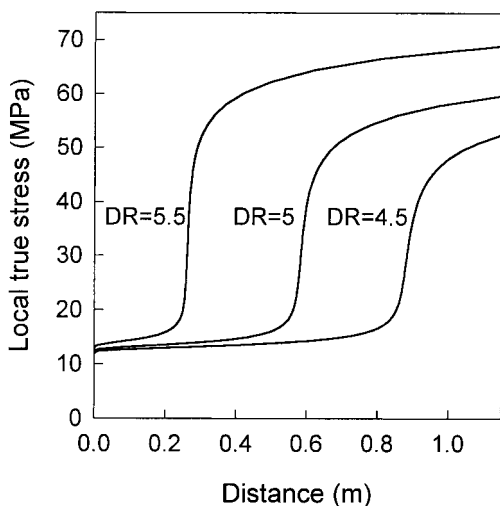


Figure 6 The calculated local true stress distribution along the drawing line for a continuous drawing of PP hollow fibers at various applied draw ratios ($T = 80^{\circ}\text{C}$).

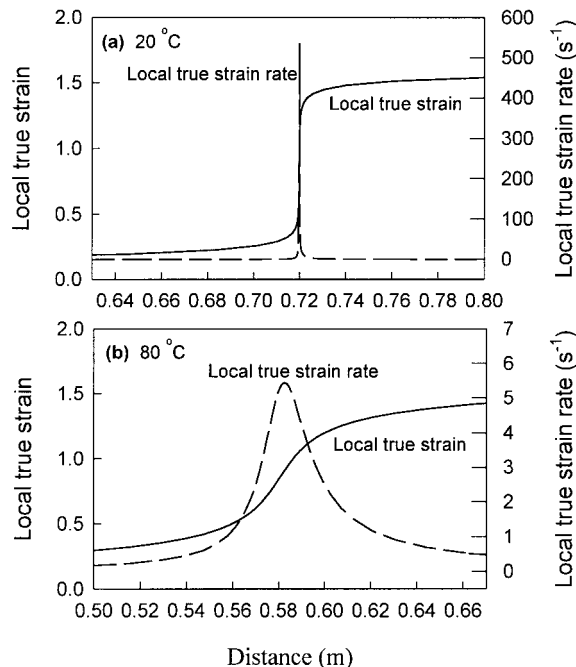


Figure 7 The predicted local true strain and strain-rate distribution along the drawing line for a continuous drawing of PP hollow fibers at two drawing temperatures (DR = 5): (a) $T = 20^{\circ}\text{C}$; (b) $T = 80^{\circ}\text{C}$.

aspect ratio (i.e., the x axis of curves in Fig. 7 is enlarged), but at a lower drawing temperature the plastic instability obviously appears. The apparent neck profile at a lower temperature (20°C) was observed in experiments, as will be shown later. The formation of a neck with the drawing temperature can be analyzed by considering the dependence of strain-rate sensitivity on temperatures. It may be inferred that strain-rate sensitivity of solid polymers increases with temperature by considering that the strain rate is a more significant factor than strain for the change in stress at high temperatures (for extreme cases, polymer melts at the temperature above the melting point in the spinning process can be successfully analyzed by the rheological relation with only a strain rate dependence, e.g., Newtonian fluid). We can, thus, assume that the strain-rate sensitivity parameter increases with temperature, as shown in G'Sell's data.¹² As a consequence, this affects the deformation behavior in the drawing process. Similar consideration can be found in Coats and Ward's work.¹⁵ high strain-rate sensitivity implies that a large change in stress is required for a small change in the strain rate. In other words, a small increase of the stress

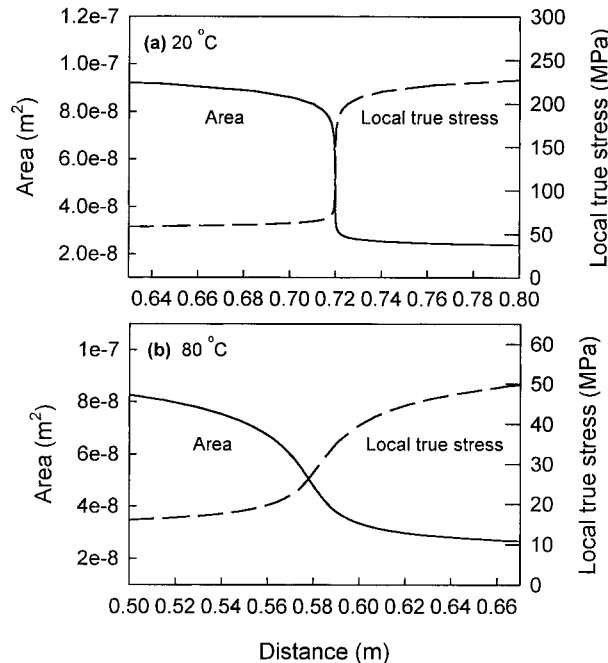


Figure 8 The predicted area and local true stress distribution along the drawing line for a continuous drawing of PP hollow fibers at two drawing temperatures (DR = 5): (a) $T = 20^\circ\text{C}$; (b) $T = 80^\circ\text{C}$.

cannot produce a large change in the strain rate, and so an increase of the strain-rate sensitivity causes homogeneous deformation. Their discussion is in qualitative accordance with the results of this study in that the strain-rate sensitivity parameter, m , is chosen as a higher value with increasing temperature, which makes the deformation more homogeneous with increasing the drawing temperature.

The position of the strain localization is a function of the draw ratio, as described above, and the inflection point is less sensitive at a higher drawing temperature, as presented in Figure 9. It shows that the position of inflection point at 20°C is so sensitive to the draw ratio that necking occurs unrealistically near the initial position in the drawing line for an applied draw ratio of 6. However, experiments conducted at 20°C did not show this calculated result, but breakage of filaments occurred during drawing at the highest draw ratio at this temperature instead of the appearance of a strain localization near the feed roll.

The drawing force is an important characteristic of a continuous drawing related to the deformation kinetics and texture of the drawn fibers. However, the drawing force associated with a par-

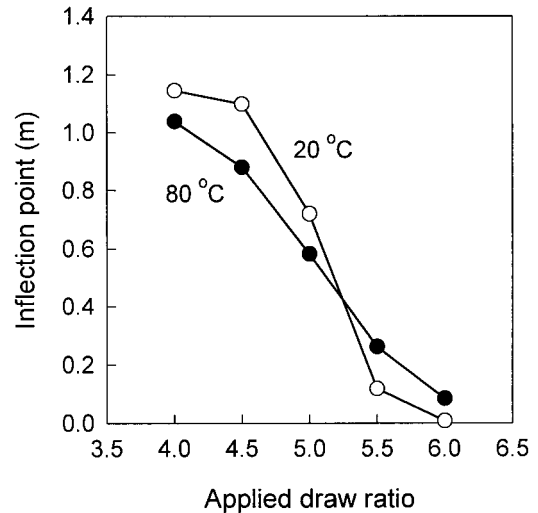


Figure 9 The calculated positions of inflection points with the applied draw ratio for a continuous drawing of PP hollow fibers at two drawing temperatures: $T = 20^\circ\text{C}$ (○); 80°C (●).

ticular set of drawing conditions is, in general, unknown, and this is a factor that makes it difficult to analyze deformation in the roll drawing.¹⁰ In this study, the drawing force can be obtained by calculation, and it is plotted as a function of the applied draw ratio at two drawing temperatures, as in Figure 10. According to the results shown in Figure 10, the drawing force increases with the applied draw ratios, as expected. In this

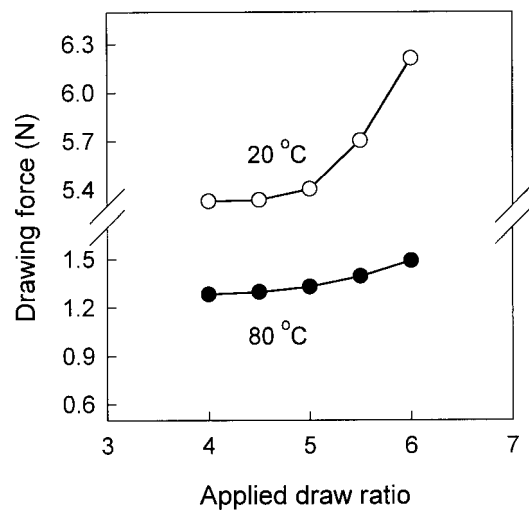


Figure 10 The calculated drawing forces with the applied draw ratio for a continuous drawing of PP hollow fibers at two drawing temperatures: $T = 20^\circ\text{C}$ (○); 80°C (●).

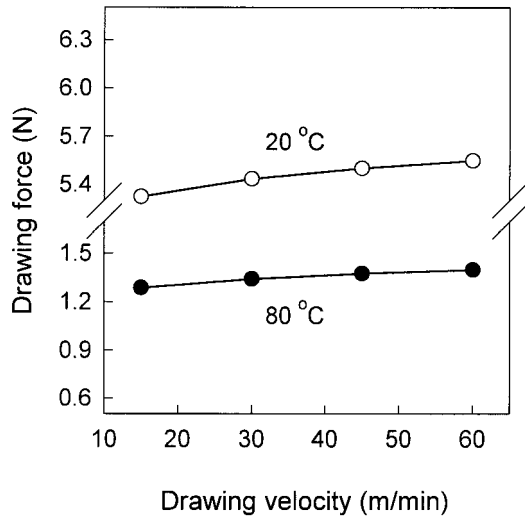


Figure 11 The calculated drawing forces with the drawing velocity for a continuous drawing of PP hollow fibers at two drawing temperatures (DR = 5): $T = 20^\circ\text{C}$ (○); 80°C (●).

plot, the slope of the curves increases steeply at a certain draw ratio, and this feature is more apparent at a lower temperature. Such a tendency can also be found in other experimental data,^{8,9} and is considered to be related with a natural draw ratio: the steep slope above a draw ratio corresponding to a natural draw ratio results from an increase of the drawing force along the drawing line due to the dominance of strain-hardening effects.

The effects of the drawing velocity were also investigated. The predicted results indicate that the drawing velocity or average strain rate exhibits less influence on the drawing force compared with the draw ratio and temperature (Fig. 11).

For verification of predicted results, tension and neck geometry were measured, as shown in Figures 12 and 13. Figure 12(a) illustrates that the tension increases with the applied draw ratio, and the rise in slope is also found with the calculated results (Fig. 10). The result for the temperature dependence of tension indicates that the overall tension along the drawing line decreases as the drawing temperature increases [Fig. 12(b)]. Figure 12(c) shows that the effect of drawing velocity on tension is similar to the calculated results (Fig. 11).

The necking phenomena at different temperatures are described by the profiles of the outer diameters at the positions of the most remarkable

diameter reduction (Fig. 13). It is shown that the neck profile becomes sharper as the drawing temperature decreases. The shallow neck at higher drawing temperatures indicates that strain is not localized intensively at the necking point, but distributed along the drawing line. At 80°C , the evidence of a neck is not observed, due to an almost homogeneous deformation.

A hollow fiber has a unique structure that is distinguished from circular fibers, and the properties, as a result of such structural features, are better developed as hollowness increases. The change of hollowness of the drawn fibers was investigated by experiments, and this is shown in Figure 14. According to this result, it decreases

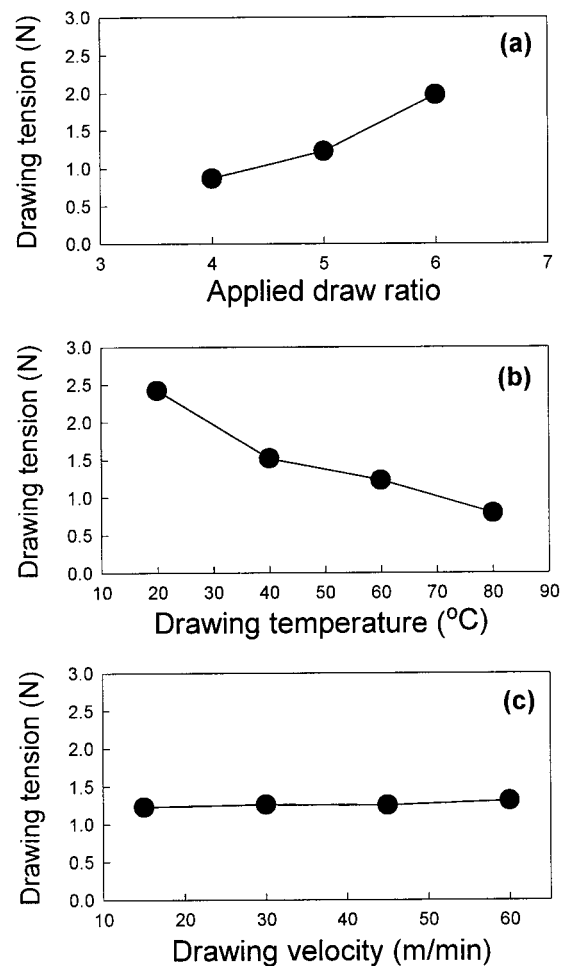


Figure 12 Measured drawing tensions of PP hollow fibers continuously drawn for various conditions: (a) for an applied draw ratio ($T = 80^\circ\text{C}$); (b) for a drawing temperature (DR = 5); (c) for a drawing velocity ($T = 80^\circ\text{C}$, DR = 5).

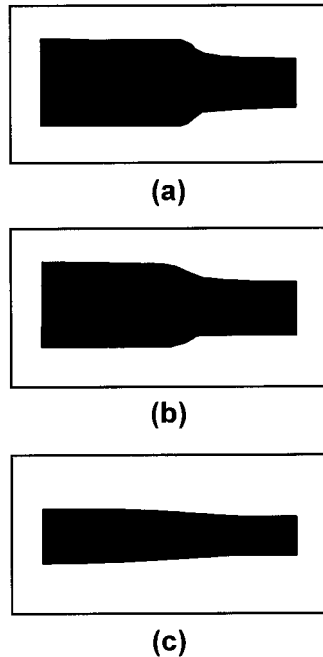


Figure 13 Neck profiles of PP hollow fibers captured from the region of strain localization in the drawing line at three drawing temperatures (DR = 5): (a) 20°C; (b) 40°C; (c) 60°C.

with increasing temperature, as in the melt-spinning process.³

The hollowness of drawn fibers is influenced by the change in the inner and outer diameters during the drawing process. It is worth noting that the hollowness of fibers drawn at 30°C is higher than that of the undrawn fibers, whereas it is lower at higher drawing temperatures. This result implies that at 30°C the decrease in the outer diameter is larger than that for the inner diameter, and then the hollowness of the final drawn fibers is higher than that of the undrawn fibers. However, at drawing temperatures above 30°C, the decrease in the inner and outer diameters along the drawing line seems to occur in a similar ratio, due to the fact of a lower hollowness of the drawn fibers than that of the undrawn fibers. In conclusion, the stretching of hollow fibers results in the decrease of hollowness during melt spinning and drawing at high temperatures when the deformation occurs without intensive strain localization. On the other hand, at 30°C the hollowness of the fiber increases along the drawing line where a sharp neck can be observed. It can be found from these results that the process conditions in the continuous drawing of hollow fibers

have an influence not only on the deformation kinetics but also the profile development of hollow fibers.

CONCLUSIONS

It has been shown that the combination of some governing equations with the constitutive relation for solid polymers that can describe the true (stress-strain-strain rate) surface makes it possible to express the deformation behavior of continuous drawing, which can be simplified by the assumption of a constant force and isothermal conditions. The drawing conditions, such as an applied draw ratio, drawing temperature, and drawing velocity, affect the deformation behavior of hollow fibers along the drawing line. It has also been shown that increasing the applied draw ratio and decreasing the drawing temperature result in the increase intensity of strain localization and drawing force, but drawing velocity has less effect on the drawing force. The manner of deformation, according to the drawing temperature, affects the evolution of hollowness during stretching in a continuous drawing process. The drawing of hollow fibers at 30°C results in higher hollowness but lower than that of undrawn fibers above this temperature.

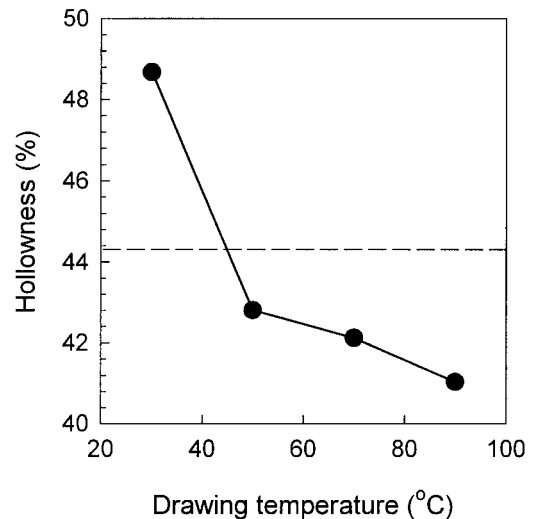


Figure 14 Measured hollowness of the drawn fibers as a function of drawing temperature. Horizontal dashed line indicates hollowness of the undrawn fibers (DR = 5).

This work was supported by the Research Fund for Advanced Materials (in 1997) of the Ministry of Education, the Republic of Korea.

REFERENCES

1. Cabasso, I. *Hollow Fiber Membr Encyclopedia Chem Technol* 1981, 12, 492.
2. Kim, J. J.; Jang, T. S.; Kwon, Y. D.; Kim, U. Y.; Kim, S. S. *J Membr Sci* 1994, 93, 209.
3. Oh, T. H.; Lee, M. S.; Kim, S. Y.; Shim, H. J. *J Appl Polym Sci* 1998, 68, 1209.
4. Kase, S.; Matsuo, T. *J Polym Sci Part A* 1965, 3, 2541.
5. Goerge, H. H. *Polym Eng Sci* 1982, 22, 292.
6. Cao, J.; Kikutani, T.; Takaku, A.; Shimizu, J. *J Appl Polym Sci* 1989, 37, 2683.
7. Denton, J. S.; Cuculo, J. A.; Tucker, P. A. *J Appl Polym Sci* 1995, 57, 939.
8. Ziabicki, A. *Fundamentals of Fiber Formation*; Wiley-Interscience: London, 1976.
9. Le Bourvellec, G.; Beautemps, J.; Jarry, J. P. *J Appl Polym Sci* 1990, 39, 319.
10. Salem, D. R. ANTEC '96 1996, 1725.
11. Le Bourvellec, G.; Beautemps, J. *J Appl Polym Sci* 1990, 39, 329.
12. G'Sell, C.; Marquez-Lucero, A. *Polymer* 1993, 34, 2740.
13. G'Sell, C.; Hiver, J. M.; Dahoun, A.; Souahi, A. *J Mater Sci* 1992, 27, 5031.
14. G'Sell, C.; Jonas, J. J. *J Mater Sci* 1981, 16, 1956.
15. Coates, P. D.; Ward, I. M. *J Mater Sci* 1980, 15, 2897.
16. Haward, R. N. *J Polym Sci Polym Phys Ed* 1995, 33, 1481.
17. Guan, J. Y.; Saraf, R. F.; Porter, R. S. *J Appl Polym Sci* 1987, 33, 1517.